Article:
Demir, E., Eltes, P., Castro, A.P.G. et al. (2020) Finite element modelling of hybrid stabilization systems for the human lumbar spine. Proceedings of the Institution of Mechanical Engineers, Part H: Journal of Engineering in Medicine, 234 (12). pp. 1409-1420. ISSN: 0954-4119

https://doi.org/10.1177/0954411920946636

Demir E, Eltes P, Castro AP, Lacroix D, Toktaş İ. Finite element modelling of hybrid stabilization systems for the human lumbar spine. Proceedings of the Institution of Mechanical Engineers, Part H: Journal of Engineering in Medicine. 2020;234(12):1409-1420. doi: https://doi.org/10.1177/0954411920946636.

Finite Element Modelling of Hybrid Stabilization Systems for the Human Lumbar Spine

E. DEMIR[1*], P. ELTES[2], A. P. G. CASTRO[3], D. LACROIX[4], I. TOKTAS[1]

[1]Mechanical Engineering Department, Ankara Yildirim Beyazit University, Ankara, Turkey.
[2]National Center for Spinal Disorders, Budapest, Hungary.
[3]IDMEC, Instituto Superior Técnico, Universidade de Lisboa, Lisbon, Portugal.
[4]INSIGNEO Institute for in Silico Medicine, University of Sheffield, Sheffield, United Kingdom.

Abstract

Intersomatic fusion is a very popular treatment for spinal diseases associated with intervertebral disc (IVD) degeneration. The effects of three different hybrid stabilization systems (HSS) on both Range of Motion (ROM) and intradiscal pressure (IDP) were investigated, as there is no consensus in the literature about the efficiency of these systems. Finite Element (FE) simulations were designed to predict the variations of ROM and IDP from intact to implanted situations. After HSS implantation, L4-L5 level did not lose its motion completely, while L5-S1 had no mobility as a consequence of disc removal and fusion process. BalanC HSS represented higher mobility at index level, reduced intradiscal pressure of adjacent level, but caused to increment in ROM by 20% under axial rotation. Higher tendency by 93% to the failure was also detected under axial rotation. Dynesys HSS represented more restricted motion than BalanC, and negligible effects to the adjacent level. B-DYN HSS was the most rigid one among all three systems. It reduced IDP and ROM at adjacent level except from motion under axial rotation being increased by 13%. Fracture risk of B-DYN and DTO components was low when compared with BalanC. Mobility of the adjacent level around axial direction should be taken into account in case of implantation with BalanC and B-DYN systems, as well as on the development of new designs. Having these findings in mind, it is clear that hybrid systems need to be further tested, both clinically and numerically, before being considered for common use.

Keywords: Lumbar spine, finite element modelling, range of motion, hybrid stabilization, intradiscal pressure.

Contact information of the corresponding author:
Eylul Demir, Faculty of Engineering and Natural Sciences, Ankara Yildirim Beyazit University, 06010, Ankara, Turkey.
Phone: 00903129062229, e-mail: edemir@ybu.edu.tr

ORCID information:
E. DEMIR - https://orcid.org/0000-0003-1478-1875
P. ELTES - https://orcid.org/0000-0002-4377-8635
A. P. G. CASTRO - https://orcid.org/0000-0002-6130-0408
D. LACROIX - https://orcid.org/0000-0002-5482-6006
I. TOKTAS - https://orcid.org/0000-0002-4371-1836

1. Introduction

Low back pain is the second most common musculoskeletal disease[1] and generally can be attributed to the degeneration of the lumbar intervertebral disc (IVD). Early to mild cases of disc degenerative disease (DDD) can be treated by non-surgical methods such as bed rest and physiotherapy exercises while severe ones require surgical operations.[2] Spinal fusion provided by rigid stabilization has been considered as the gold standard for the operation of DDD[3,4], however it was observed that it could lead to the adjacent segment disease.[5,6] General causes of the adjacent segment diseases (ASD) are attributed to the increased motion and changing the instantaneous centre of rotation.[7] The clinical reports regarding that the ASD can be occurred in the range of 12.2% to 35% after fusion operation.[8,9]

Hybrid stabilization systems (HSS) can be effective in multilevel DDD that these systems have been developed to protect the adjacent segment from excessive mobility after spinal fusion.[10,11] HSS includes fusion with rigid instrumentation at severe DDD level and non-fusion with dynamic stabilization at the level presenting mild DDD. The level suffering from severe DDD is fused and implanted with rigid rods. The symptoms of the adjacent level are not

severe enough to warrant the arthrodesis, therefore dynamic implantation is preferred and preserves this level from hypermobility.[12] Nevertheless, clinical applications and numerical analysis of hybrid systems are very limited and requires further studies.

Detailed investigation on biomechanics of the lumbar spine requires the use of advanced computer techniques for both geometric reconstruction and stress analysis.[13] 3D reconstruction is obtained by converting medical examinations, such as Computerized Tomography (CT) images to three dimensional (3D) models. This method avoids the elimination of crucial features for the modelling of anatomical parts.[14] Over the last few decades, the Finite Element (FE) method became a preferable option for predictions of spinal stability in case of intact or implantation, as this technique can provide an insight to the tissues that in vivo and in vitro experiments are not able to reach.[15-20] FE models are also an effective and low-cost method to assess the stabilization systems for pre- and post-operative surgical treatments, as they are able to provide multiparametric analyses for different clinical scenarios.[10,21,22]

A simplified model of the most recent HSS, the commercially available Dynesys Transition Optima (DTO, from Zimmer Biomet, USA), was used in this study and compared with another two commercially available HSSs named as CD Horizon® BalanC™ (Medtronic, USA) and B-DYN® (S14 Biospine Implants SAS, France) HSSs. HSSs were designed to establish a mobile load transfer and to control motion of the segment in all loading directions, being suggested as an alternative method to multilevel lumbar arthrodesis due to the properties like its efficacy and reliability. Initial lumbar lordosis and Range of Motion (ROM) were preserved, and favourable clinical outcomes were obtained after hybrid surgery, and also DDD at the adjacent segment of the HSS may be delayed. It is possible to find many studies in the literature regarding traditional fusion treatments with rigid fixations and dynamic stabilizations at one level, but deeper or longer-term knowledge about HSS is limited. In other words, clinical and numerical significance of HSS is still unclear due to the lack of conclusive data.

The primary objective of this study is to assess the variations of ROM, intradiscal pressure (IDP) at index and adjacent levels and stress distributions of three simplified models inspired by DTO, CD Horizon® BalanC™ and the B-DYN® HSSs.

2. Materials and Methods

2.1. FE Model Creation

The lumbar spine is composed of five lumbar vertebrae (L1-L5) that are connected by facet joints, and each pair of vertebrae are separated by an IVD. In addition, seven different ligaments spread over the lumbar spine. IVD, facet joints, and ligaments are the most important load transformation segments of the lumbar spine and mechanical properties of these parts play an important role on the spinal stability. Ligaments and discs have soft and flexible structures, when compared to the vertebral bodies.[23-24]

The Quantitative Computed Tomography (QCT) images of a 39 years old female subject with two level disc degeneration at L4-S1 (Pfirmann grade III on L4-L5 and Pfirmann grade IV on L5-S1) were obtained from a Hitachi Presto CT machine (National Center for Spinal Disorders of Budapest, Hungary). CT images were reconstructed 1.25 mm slice thickness for a voxel size of 0.6 x 0.6 x 0.6 mm. Vertebral body and posterior elements were directly segmented from the CT images.[25-26] 3D Slicer, free open-source software, was used in processing of CT images.

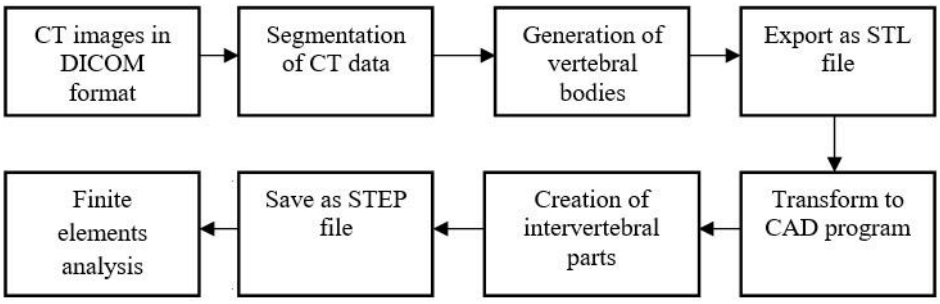

Figure 1. Flow chart of the reconstruction of lumbar spine

After exporting the model in STL (Stereolithography) format, CAD program named as Fusion 360 was used for further processing. In Fusion 360, smoother surface was obtained and finally 0.5 mm cortical thickness[25-26] was created over cancellous bone. A simplified model of S1 was created as a cubic solid.[7] Reconstruction steps of the lumbar spine are given in Figure 1.

The IVDs are divided into four parts: nucleus pulposus (NP), annulus fibrosus (AF), inferior endplate (IP) and superior endplate (SP).[15] The NP was 30-50% of the total IVD volume[27] and thickness of the cartilage endplates was 0.6 mm[28]. The main components of the vertebral coloumn are shown in Figure 2(a). Lumbar spine has seven different ligaments in real anatomy as following: anterior longitudinal ligament (ALL), posterior longitudinal ligament (PLL), ligamentum flavum (FL), intertransverse ligament (ITL), interspinous ligament (ISL), supraspinous ligament (SSL), capsular ligament (CL). Spinal ligaments have a restriction effect on spinal motion. Each ligament with linear elastic and tension only behavior was modelled in ABAQUS(R) 6.14 (Dassault Systèmes Simulia Corp., USA). Although ligaments represent nonlinear elastic behaviour in reality, they were created in a simplier way. Material properties and cross-sectional areas were adopted from literature as given in Table 1.

Three different HSS were created from the commercially available models used in clinical treatments. All of them has rigid part and dynamic part. First system has similar mechanical design with Dynesys Transition Optima® (DTO) HSS whose dynamic part is composed of Polycarbonate Urethane (PCU) spacer, Polyethylene Terephthalate (PET) cord and rigid part is composed of titanium rods as seen in Figure 2(b). Second one represents the similar mechanical properties with CD Horizon® BalanC™ HSS that is made of C shaped silicone spacer and Polyetheretherketone (PEEK) in its dynamic portion, while the fusion portion is entirely made of PEEK (Figure 2(c)). The third one is similar with B-DYN system having viscoelastic damping technology in dynamic part (Figure 2(d)). Rods are made of Titanium for both rigid and dynamic portions. Titanium screws had a mean diameter of 5.5 mm and rigid rod had diameter of 6 mm. Screw lengths were 45 mm. The thread on the pedicle screws was underestimated[29-32] to reduce the computational weight of the models. The 'tie' constraint was created between the pedicle screws and the vertebraes to be permanently bonded together by full constraint. AutoCAD Fusion 360 (Autodesk, USA) program was used for modeling of the implant components whose dimensions were taken from the product catalogues. Fusion mass properties were assigned the same as posterior elements.[33] Linear isotropic material properties were assigned to all the segments (references are provided in each entry of the Table 1). For mesh sensivity, three different mesh densities as coarse (17557 nodes, 50036 elements), medium (57238 nodes, 131756 elements) and fine (101886 nodes, 183031 elements) were analysed. The model comprising coarse elements was disregarded since it caused to excessive element distortion. Under flexion, extension and lateral bending, mesh density affected ROM values by max. 5%. Therefore, medium mesh was preferred for analyses. Total number of elements over the implanted spine was approximately 161,000 comprising tetrahedral and hexahedral element types. S1 segment was fixed.[34-36] Pure moments were applied from superior surface of L1 vertebrae as 7.5 and 10 Nm to be able to validate the model by comparing with in vitro tests. For the implanted model, L4-L5 level was implanted dynamically and L5-S1 level was subjected to fusion and fixed with the rigid stabilization. Facet joint interactions were defined as surface to surface frictionless, hard contact. General static analysis option was selected for a time period of 1 second. ROM valaues under different moments, flexion (FL), extension (EXT), lateral bending (LB) and axial rotation (AR), were calculated and IVD pressures and stress distribution over the implants were investigated. For validation the computed ROM and IDP values were compared with in vitro and other finite element method FEM studies.

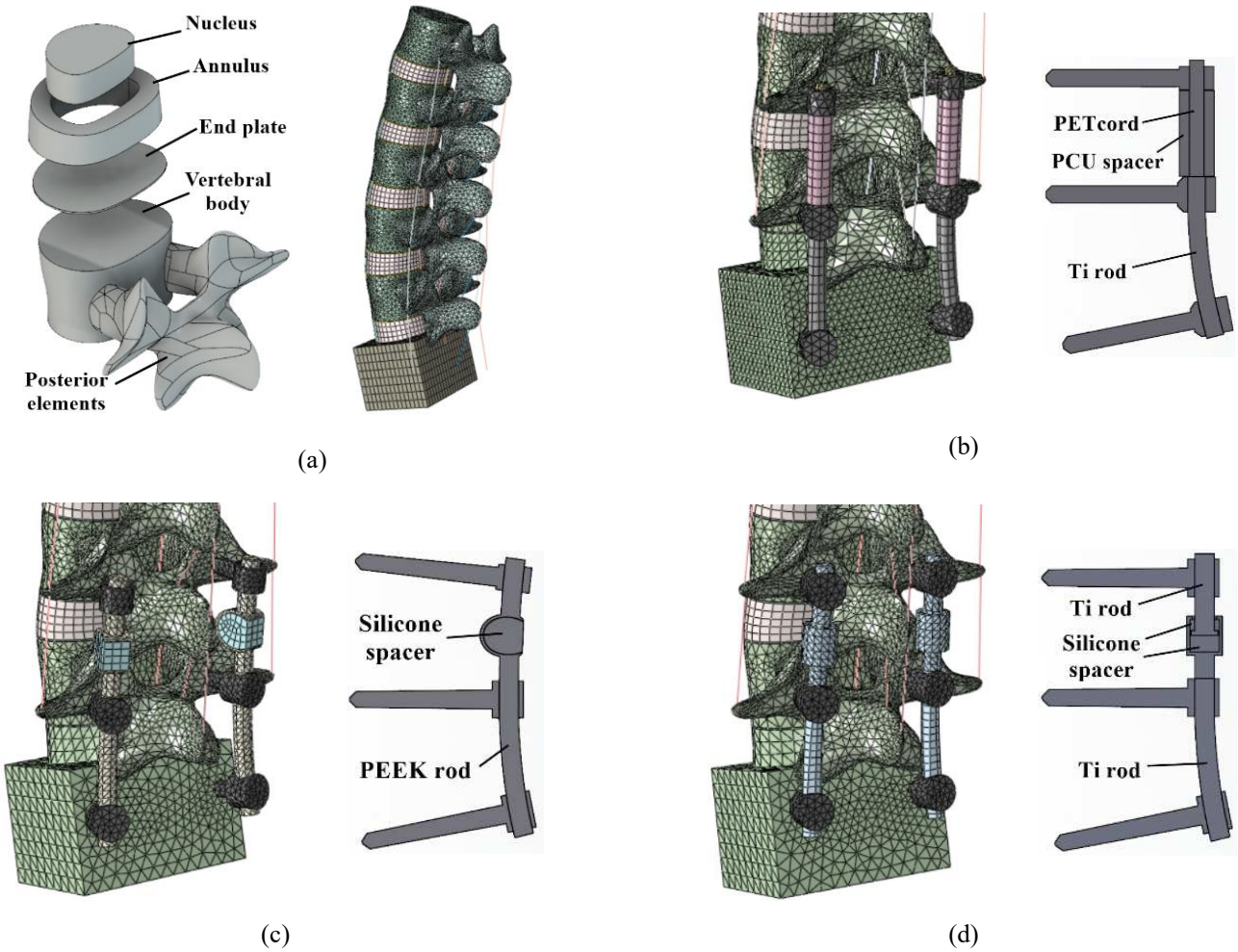

Figure 2. a) 3D model of vertebral body, b) DTO, c) BalanC and d) B-DYN

Table 1. Material properties of lumbar spine and HSSs

Material	Modulus of Elasticiy (MPa)	Poisson ratio, v	Reference
Cortical bone	12000	0.3	Shin et al.[37]
Cancellous bone	100	0.2	
Posterior elements	3500	0.25	Rohlman et al.[38]
Annulus disc	8.4	0.45	Shin et al. 2007[37]
Nucleus disc	1	0.49	
IP and SP	24	0.4	
Facet Cartilage	Hyperelastic Neo-Hookean C10=2, D1=0		Noailly et al.[39]
ALL	20		Zhong et al.[40]
PLL	20		
FL	19.5		
ITL	58.7		
ISL	11.6		
SSL	15		
CL	32.9		
PCU Spacer	68.4	0.4	
PET cord	1500	0.4	

Ti alloy rod	110000	0.3	Liu et al.[29]
Ti alloy pedicle screw	110000	0.3	
Silicone	50	0.49	https://www.azom.com[41]
PEEK	3500	0.3	Biswas et al.[42]

3. Results

3.1. ROM Analysis of Intact Spine

ROM values at each lumbar level (L1-L5) for intact model in FL, EXT, LB and AR were evaluated and given in the Table 2. Firstly, these values of the intact spine were compared with in vitro studies conducted by Yamamoto et al.[43] and Schmoelz et al.[44] who used pure bending moments of 10 Nm without any compressive load similar with current study. Yamamoto et al.[43] tested L1-L5 segments of the spine while Schmoelz et al.[44] used only L2-L4 segments. Our model results are more consistent with the latter one by considering L2-L3 and L3-L4 levels. Schmoelz's study[44] revealed a range of the rotational degrees in which our results managed to remain. However, Yamamoto's values[43] are a little higher than current findings for L1-L2 and L4-L5 levels. In the second step of the validation process, 7.5 Nm pure moment was applied to be able to make comparison with the study carried out by Dreischarf et al.[20]. They gathered data from well-established eight FE models in literature and global movement of L1-L5 body was handled. In Figure 3, red bar represents the mean value of in vitro studies, while the green bar denotes the mean value of FE studies consisting of models numbered from 1 to 8. Current model performs 33° where median value of the FE models is approximately 34° with a range of 24°-41° and in vitro tests perform 31° in the range of 23.5°- 37° in flexion-extension. Our model performs a movement of 33° where median value of the FE models perform about 35° in the range of 25°- 41° and in vitro tests shows 34° in the range of 23°- 44.5° in both of right and left lateral bending. Our model represents a rotation of 12° where median value of the FE models perform about 17° in the range of 11° - 22° and in vitro tests shows 12° in the range of 10°- 19.5° in both of right and left axial rotation.

Table 2. ROM values of intact spine

10 Nm pure moment		**L1-L2**	**L2-L3**	**L3-L4**	**L4-L5**
FL	This study	3.9	4.1	4.7	5.2
	Yamamoto et al.[43]	5.8±0.6	6.5±0.3	7.5±0.8	8.9±0.7
	Schmoelz et al.[44]	-	4.3±1.0	5.0±1.0	-
EXT	This study	3.4	3.0	3.7	4.7
	Yamamoto et al.[43]	4.3±0.5	4.3±0.3	3.7±0.3	5.8±0.4
	Schmoelz et al.[44]	-	4.6 ± 2.2	4.0±1.3	-
LB	This study	4.1	4.1	4.5	4.0
	Yamamoto et al.[43]	5.2±0.4 (R) 4.7±0.4 (L)	7.0±0.6 (R) 7.0±0.6 (L)	5.8±0.5 (R) 5.7±0.3 (L)	5.9±0.5 (R) 5.5±0.5 (L)
	Schmoelz et al.[44]	-	5.4 ± 2.2	4.7 ± 2.0	-
AR	This study	1.5	1.6	1.4	1.6
	Yamamoto et al.[43]	2.0±0.6 (R) 2.6±0.5 (L)	3.0±0.4 (R) 2.2±0.4 (L)	2.5±0.4 (R) 2.7±0.4 (L)	2.7±0.5 (R) 1.7±0.3 (L)
	Schmoelz et al.[44]	-	1.0 ± 1.0	1.0±0.6	-

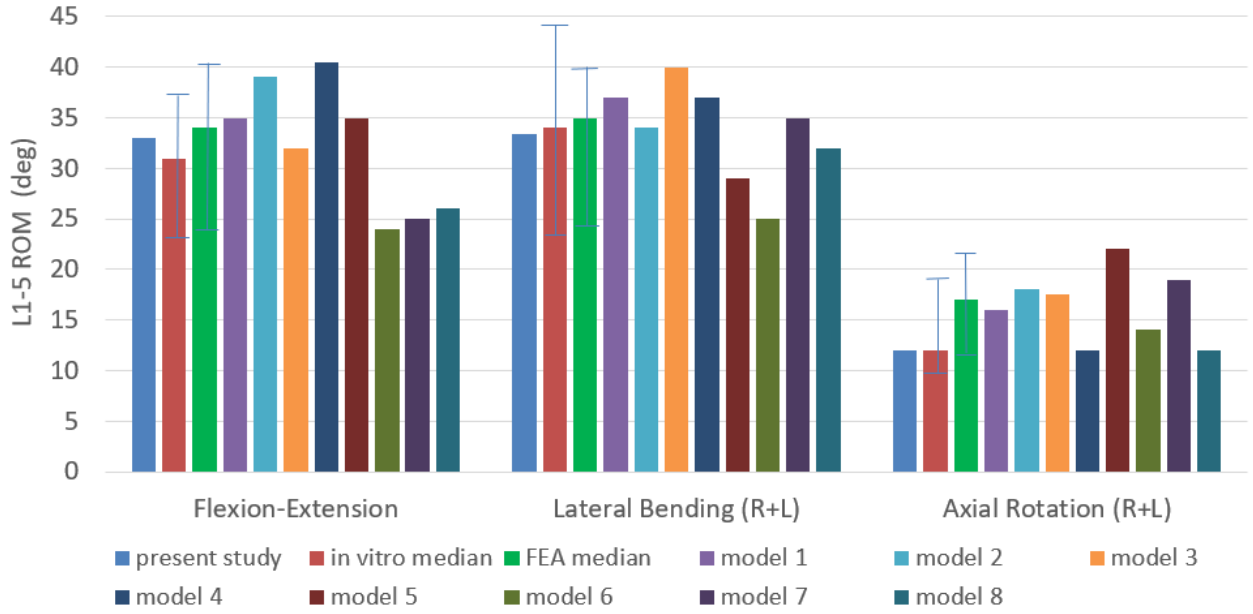

Figure 3. Comparison of ROM values under 7.5 Nm pure moment (Adapted from Dreischarf et al.[20])

3.2. ROM Analysis of Implanted Spine

There are limited FEA and in vitro studies subjected to hybrid stabilization examining the variation of ROM values especially at the level of L4-S1. Niosi et al.[45] and Cheng et al.[46] carried out in vitro studies examining ROMs of implanted spine with Dynesys by applying 7.5 Nm and 6 Nm bending moments, respectively. In those studies, as expected, ROMs at implanted level under FL, EXT, LB and AR decreased in comparison to intact spine (Table 3). Niosi et al[45] found that the mobility under FL, EXT and LB could be saved as 27%, 33%, 26%, respectively. AR capability was remained higher than others as 76%. Cheng et al.[46] showed that 26% of the mobility of both FL and EXT were saved while 41% of lateral and 85% of axial motion were preserved. Herren et al.[47] tested L2-L5 human cadaveric spine by applying 7.5 Nm pure moment and implanted BalanC to L3-L5 segments. The preservation of the motion was found as 36% in FL-EXT, 38% in LB and 82% in AR at the implanted level dynamically (L3-L4). In the current study, motion of L4-L5 level was not completely lost in all HSSs, and L5-S1 did not perform any (micro-) movement after the fusion procedure. For DTO, 13% of FL, 10% of EXT and 25% of LB motion were computed on L4-L5 level, but 81% of AR was held and found as less restricted in comparison with other rotational directions. For BalanC, it was found that 15% of FL, 13% of EXT, 33% of LB and 81% of AR were saved at L4-L5 level. For B-DYN system, 12% of the FL, 8% EXT and 24% of the LB and 52% of the AR were maintained at L4-L5 level. There was no motion at the L5-S1 level, as it was rigidly fixed, therefore the results were excluded from Table 3 for the sake of simplicity.

Table 3. ROM values of implanted spine

	L2-L3 LEVEL			L3-L4 LEVEL			L4-L5 LEVEL		
	Int.	**Ins.**	**%**	**Int.**	**Ins.**	**%**	**Int.**	**Ins.**	**%**
FL									
B-DYN							5.2	0.6	12
BalanC								0.8	15
DTO (this study)								0.65	13
Dynesys (Niosi et al.)				3.7 ± 1.5	1 ± 0.6	27			
EXT									
B-DYN							4.7	0.36	8
BalanC								0.62	13
DTO (this study)								0.48	10
Dynesys (Niosi et al.)				3.3 ± 1.5	1.1 ± 0.7	33			

FL/EXT									
Dynesys (Cheng et al.)	4.6 ± 2.9	1.2 ± 0.5	26						
BalanC (Herren et al.)						36			
LB									
B-DYN							4.0	0.95	24
BalanC								1.3	33
DTO (this study)								1.0	25
Dynesys (Niosi et al.)				7.6 ± 2.8	2 ± 1	26			
Dynesys (Cheng et al.)	5.7 ± 3.6	2.34 ±0.79	41						
BalanC (Herren et al.)						38			
AR									
B-DYN							2.1	1.1	52
BalanC								1.7	81
DTO (this study)								1.7	81
Dynesys (Niosi et al.)				4.2 ± 1.8	3.2 ± 2	76			
Dynesys (Cheng et al.)	3.5 ± 1.7	3.0 ± 1.3	85						
BalanC (Herren et al.)						82			

ROM: range of motion; FL: flexion; DTO: Dynesys Transition Optima; EXT: extension; LB: lateral bending; AR: axial rotation
This study, pure moment of ± 10 Nm
Niosi et al.[45] n = 10, L3-L4 level, pure moment of ± 7.5 Nm
Cheng et al.[46] n = 6, L3-L4 level, pure moment of ± 6 Nm
Herren et al.[47] (2017) n=1 L2-L5 level, pure moment of ± 7.5 Nm
% = ($ROM_{implanted}$/ROM_{intact}) x 100, (n=number of cadaveric samples)

Figure 4 represents the variations of motion at adjacent level (L3-L4) after implantation. The incremenets in ROM were evaluated as 3% for EXT of B-DYN, and 2% for LB of DTO that both might be considered insignificantly. Under AR, ROM of BalanC and B-DYN were increased by 20% and 13%, respectively.

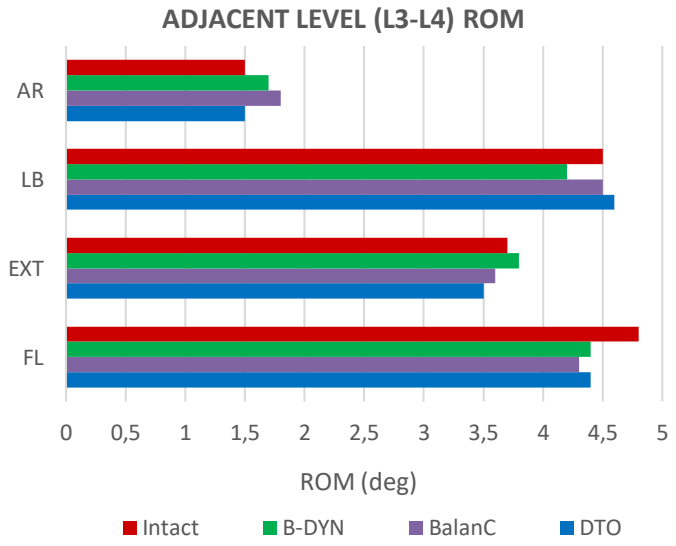

Figure 4. ROM values at adjacent level

3.3. IDP Analysis of Intact and Implanted Spine

The mobility of L5-S level is approximately zero as these segments were fused to each other. IDP at index (L4-L5) and adjacent level (L3-L4) of the intact spine were addressed and variations were evaluated under pure moment of 10 Nm without any follower load. As expected, implantation has reduced the IDP at index level due to the descending load over it. In addition, dynamic part of HSS prevented excessive IDP at adjacent level. Figure 5 (a) represents the pressure distributions at adjacent level and 5 (b) shows the pressures at index level. In order to compare with in vitro studies, only nucleus part was handled[48-50]. The maximum pressure was found as 0.29 MPa in FL, 0.36 MPa in EXT, 0.36 MPa in LB, and 0.11 MPa in AR at adjacent level (L3-L4) of intact spine and given in Figure 5 (a). Besides, IDP decreased under all loading conditions after implantations. B-DYN and BalanC behaved similarly but caused to lower IDP values in comparison to DTO. At the index level (L4-L5) of intact case, the predicted IDPs were determined as 0.27 MPa, 0.36 MPa, 0.39 MPa and 0.12 MPa, respectively. The reduction was evaluated as 56% in FL, 92% in EXT, 85% in LB and 33% in AR with DTO implant, 59% in FL, 89% in EXT, 92% in LB, 75% in AR with B-DYN implant, 59% in FL, 94% in EXT, 79% in LB, 58% in AR with BalanC implant as seen in Figure 5 (b).

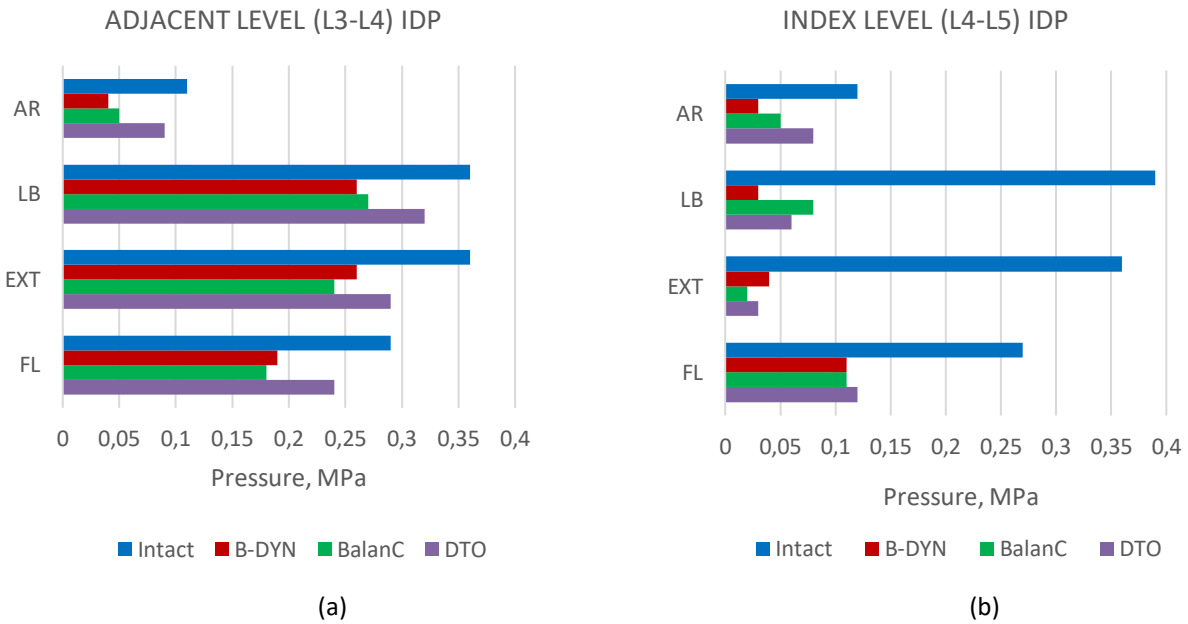

Figure 5. Comparison of intradiscal pressures of intact and implanted models at (a) adjacent (L3-L4) and (b) index (L4-L5) levels

3.1. Stress Distribution over the Hybrid Systems

Maximum Von Mises stresses (VMS) over rods and screws were evaluated seperately on account of different material strength values of those parts. Figure 6 (a) shows the graphical representation of VMS values of rods. VMS of rods of all HSSs remained under 50 MPa under FL and EXT but reached to larger values under AR that 102.6 MPa, 97.7 MPa and 150.4 MPa were obtained for DTO, BalanC and B-DYN systems, respectively. Stress distribution of DTO screws was found at lowest rates whereas B-DYN had highest VMS over the screws except FL. Maximum VMS of B-DYN screws was found as 136.3 MPa under AR and it was seen in Figure 6 (b).

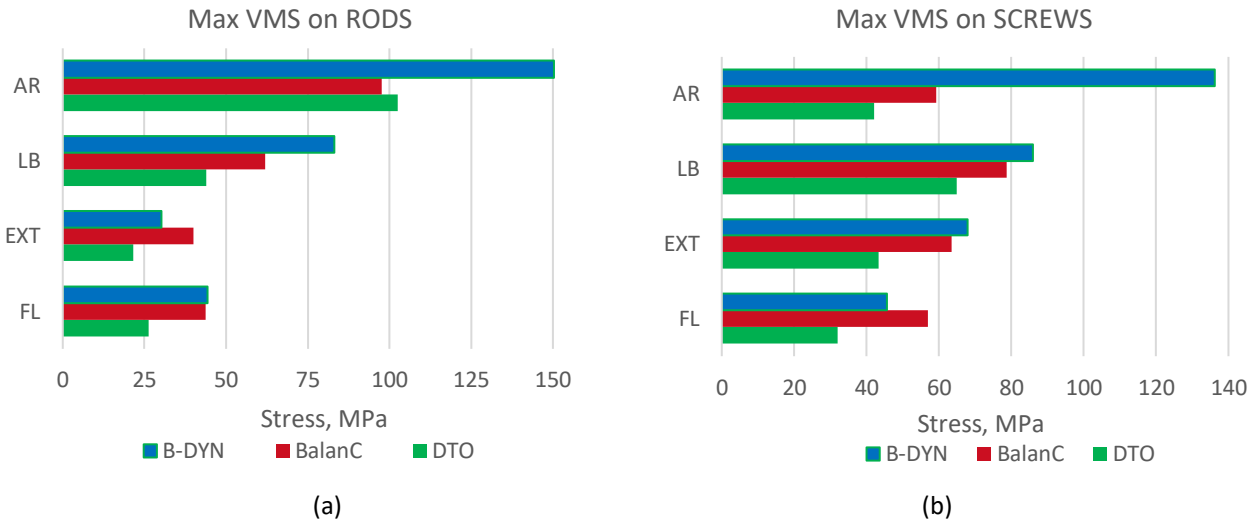

Figure 6. Comparison of maximum VMS of a) rods and (b) screws

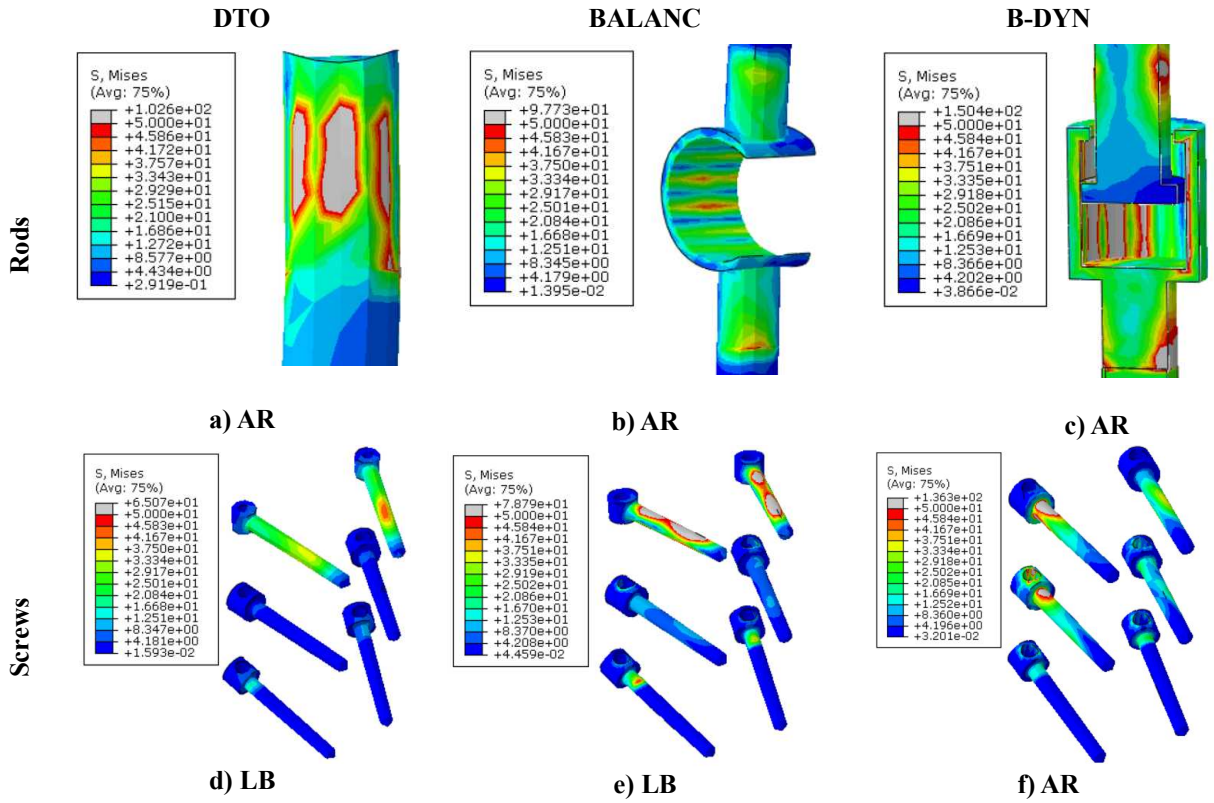

Figure 7. Maximum VMS distribution on rods of (a) DTO under AR, (b) BalanC under AR, (c) B-DYN under AR and screws of (d) DTO under LB, (e) BalanC under LB, (f) B-DYN under AR

DTO rods includes two different materials as Ti rod and PET cord, however, critical area was found as mating surface between Ti rod and screw that stress rate was notably high as given in Figure 7 (a). Maximum VMS was evaluted over C shape of BalanC that was relatively thinner as represented in Figure 7 (b). Similarly, maximum stresses distributed over Ti rods of B-DYN system where the wall thickness is thinner as seen in Figure 7(c). When screws of HSSs were handled, B-DYN, having a little more rigidity than others, was also exposed to the highest stress levels. In addition, the regions under stresses were close to the posterior elements of spine; consequently, screw heads and Ti rods were affected more. This can be attributed to the low load-sharing capability of B-DYN and loading on the posterior elements is higher

than vertebral bodies (Figure 7 (f)). On the contrary, BalanC involves more flexible rods and has more load-sharing capability over vertebral bodies. Therefore, stress increased along and towards to the end of the screws as seen in Figure 7 (e). DTO was similar with BalanC but lower VMS (Figure 7 (d)). To evaluate the risk of fracture (RF) of the implants systems, following formula where σ_{VMS} denotes maximum VMS and σ_{UTS} denotes ultimate tensile strength was used. RF is the ratio between the maximum VMS and the ultimate tensile strength of the implant materials as seen in Eq. 1.

$$RF = \sigma_{VMS}/\sigma_{\mathrm{UTS}} * 100 \qquad \text{Eq. (1)}$$

σ_{UTS} was taken as 900 MPa for Ti alloy[51] and 105 MPa for PEEK rods[52]. RF values of rods were calculated as 11% for DTO, 93% for BalanC and 17% for B-DYN systems. RF of Ti screws were found as 7% for DTO, 9% for BalanC and 15% for B-DYN systems.

4. Discussion

One can say that as the distance to the sacrum increases, a progressive movement of the vertebral bodies is increased under bending moments. At the same time, the IVD motion decreases when one goes up in the lumbar spine, from L5 to L1. Concerning the literature data, ROM values of intact spine were found to be reasonable. ROMs were occurred in the range of experimental study of Schmoelz et al.[44] where only L2-L4 segments were tested. Yamamoto's results[43] exhibited more flexible behavior than ours in all rotational directions. However, Eberlein et al.[53] stated that ROM values under flexion moments were appeared to be lower than experimental results. To strenghten the validation process, collected data from Dreischarf et al.[20] were included for comparison under 7.5 Nm pure moments. Values of current model were remained within the range of either other participating FE models or in vitro test values in terms of flexion-extension, lateral bending (right+left) and axial rotation (right+left).

Fusion has been considered as a gold standard of the treatment of spinal diseases[53,54], however ASD has occured in case of spinal fusion surgery that accelerates the degeneration at superior or inferior discs.[55-57] Aunoble et al.[1] suggested that the HSS can be an alternative to the multilevel interventions, however long term clinical studies and following-up are required for supporting the certain assessments[3,12,58] and the patient selection is also an important factor for the good functional outcomes and desired achievements.[59] Lee et al.[60] compared DTO and Nflex systems in terms of ROM. The patients were suffering from spondylolisthesis and severe disc narrowing. They found out that hybrid surgery could maintain the intersegmental motion and delaying adjacent DDD. Clinical outcomes conducted by Baioni et al.[61] obtained the satisfactory results after 5-year follow-up and found that ASD rate was as low as 10%. Maserati et al.[12] investigated the Visual Analogue Scale (VAS) in case of using DTO for arthrodesis with rigid and stabilized dynamically at adjacent level for 24 patients. Their findings were promising in terms of alleviating pain and DDD. In another study, the effects of one level and two-level implantation with DTO device was studied. DTO device was found to limit the ROM at one level with pedicle screws less rigid than conventional and, when used as in a hybrid construct, it allowed for more stability than the intact case but less than rigid fixation.[46] Strube et al.[36] suggested replacing a DTO system adjacent to a single-level fusion, thus adjacent level can be prevented from hypermobility by load-sharing and also limiting ROM of this implanted level. Formica et al.[62] get good clinical outcomes after two year follow-up forty-one patients implanted BalanC who were suffering from one level lumbar degenerative disease and initial disc degeneration at the adjacent level. No misalignment of lumbar lordosis or descending of intradiscal height was detected. Herren et al.[47] tested BalanC instrumented on five human cadaveric lumbar spines (L2 to L5) under 7.5 Nm bending moments and besides, compared with one level rigid rod. They revealed that BalanC represented similar behaviors with rigid rod even in dynamic portion but AR was found less restricted. They also stated that BalanC did not lead to any notable effects on adjacent segment under FL-EXT and AR, while lateral motion increased by 15%. In current study, superior or inferior segment to fusion was instrumented with HSSs to limit mobility and also to prevent hypermobility. The magnitude of ROM in all loading directions after HSSs implantation was significantly lower in comparison with the intact case. However, reduction was found at least in AR of index level that 52%, 81% and 81% of the mobility were preserved for B-DYN, BalanC and DTO, respectively. B-DYN system allowed less motion among all the HSSs and BalanC provided the highest mobility in index level. FL of adjacent segment L3-L4 represented similar behavior for all HSSs and was rated under intact case. Besides this, negligible deviations were detected under EXT and LB after implantations. B-DYN and BalanC caused increment by 13% and 20% of AR movement that may cause to the risk of ASD while no significance was detected for DTO. In comparison to the similar clinical findings, it seems plausible to say the low risk of ASD in case of DTO implantation.

L4-L5 and L5-S1 are the most affected segments of the DDD[15] and are also the central level under study here. Rohlmann et al.[48] calculated IDP of L4-L5 level as 0.1 MPa for FL, 0.15 MPa for EXT, 0.1 MPa for LB and 0.08 MPa

for AR under 7.5 Nm and 3.75 Nm pure moments. Wilke et al.[49] found higher values than Rohlmann's study[48] under the same moment. Approximately 0.39 MPa for FL and 0.33 MPa for EXT were obtained where L2-L3 and L4-L5 segments were included to tests. Heuer et al.[50] evaluated the IDP of L4-L5 segment as 0.35 MPa where the highest pressure was 0.40 MPa under 10 Nm FL moment. In the same way, 0.16 MPa was found under EXT where the maximum value was 0.36 MPa. In our study, IDP was 0.27 MPa for FL, 0.36 MPa for EXT, 0.39 MPa for LB and 0.12 MPa for AR at L4-L5 level under 10 Nm pure moments. To compare the previous studies, the findings seemed to be comply with current study, however, Rohlmann's results were remained lower than others.

In current study, L4-L5 level performed lower disc pressure due to HSSs implantation for all rotations in common with Liu's study[29] in which the Dynesys reduced loading on disc and facets. The reduction was evaluated as 56% in FL, 92% in EXT, 85% in LB and 33% in AR with DTO implantation, 59% in FL, 89% in EXT, 92% in LB, 75% in AR with B-DYN system, 59% in FL, 94% in EXT, 79% in LB, 58% in AR with BalanC. Schmoelz's study[63] confirmed that posterior instrumentation both EXT and LB unloads the disc. On the contrary of that, same study showed slight differences under FL and AR loading unlike our study. Schmoelz's outcomes[63] revealed negligible deviations in IDP at adjacent levels, however, current findings showed IDP was reduced remarkably especially for B-DYN and BalanC under AR that the reduction was evaluated as 64% for B-DYN system and 55% for BalanC. B-DYN and BalanC behaved similar way and caused to lower IDP values in comparison to DTO.

Kashkoush et al.[59] investigated developed infections, screw breakages and interbody cage migrations over 66 patients implanted with the DTO system for the treatment of disc herniation and spinal stenosis. Results indicated that the DTO system was reliable and viable technique and there was no higher wound infection or implant failure than conventional systems. We found that DTO provides relatively less motion in dynamic portion than BalanC, and did not create any significant change in mobility but reduction in IDP at adjacent segment. RF was evaluated as low as 11% for Ti rods and 7% for Ti screws, i.e., there results are compliant with Kashkoush's study[59]. Therefore, the induction of ASD or implant failure are still questionable under the current findings. Oikonomidis et al.[64] found ASD rate of 15% and detected high implant failure (18%) in case of using BalanC. In current study, RF values of BalanC PEEK rods and Ti screws were calculated as 93% and 9%, respectively. Rods were found to be prone to breakage that this outcome is in agreement with Oikonomidis's study[64]. To the author's best knowledge, number of clinical or numerical studies of B-DYN system is very limited, therefore further clinical studies are needed for more accurate agreements. In current stress analysis, RF was evaluated as 17% for Ti rods and 15% for Ti screws.

Excessive (micro-) mobility and high IVD pressures are undesired phenomena very frequently leading to ASD and increment in motion at adjacent level under AR is still a critical phenomena for the dynamic implantation systems. In our study, under AR, increments in ROM of B-DYN and BalanC were found as 13% and 20%, respectively. However, reasonable lower values of IDP and negligible increments (except AR) in ROM at adjacent segment were considered as acceptable conditions to prevent or delay ASD, at least for HSS implantation at L4-S1 levels. Even axial rotation may be an important point to consider, i.e., it is possible to say that the residual mobility was still in the moderate range suggested by in vitro studies. In addition, higher tendency to breakage of PEEK rod should also be considered within the product development process.

5. Conclusions

This study brings a new complete lumbar spine FE model (L1-S1) based on CT data, which is useful for further FE lumbar spine studies. The most important findings were generated when different HSSs were implanted to the L4-S1 levels: it was shown here that L4-L5 level was dynamically stabilized, not losing all of its natural motion. In addition, IDP was lower for this level, due to decreasing loads for all rotations. This resulted in not having a substantial IDP increment at L3-L4 level after stabilization, as it would be expected by the lighter restrictions imposed on L4-L5 in comparison with rigid fixation. L5-S1 level still had no mobility as a consequence of disc removal and fusion process. However, the current results showed that some important points in product design should be taken into consideration: i) less restriction capability under AR occurred after implantation is an undesired situation that may be lead to ASD later; ii) implant failure may come up due to the stress concentration over the rods of implants. Therefore, the FE analysis of the HSSs selected for this work showed that such systems could be effective for maintaining some of the natural lumbar spine motion, while reducing the probability for accelerating adjacent level degeneration, if the identified design limitations are taken into account and translated to the clinical practice.

6. Acknowledgments

A. P. G. Castro would like to acknowledge the funding from the Portuguese Science and Technology Foundation (FCT), through IDMEC, under LAETA project UIDB/50022/2020.

7. References

1. Aunoble S, Meyrat R, Al Sawad Y, et al. Hybrid construct for two levels disc disease in lumbar spine. *Eur Spine J* 2010; 19(2): 290-296.
2. Qian J, Bao Z, Li X, et al. Short-term therapeutic efficacy of the ISOBAR TTL dynamic internal fixation system for the treatment of lumbar degenerative disc diseases. *Pain Physician* 2016; 19(6): 853-861.
3. Hudson WR, Gee JE, Billys JB, et al. Hybrid dynamic stabilization with posterior spinal fusion in the lumbar spine. *SAS J* 2011; 5(2): 36-43.
4. Schwarzenbach O, Rohrbach N and Berlemann U. Segment-by-segment stabilization for degenerative disc disease: a hybrid technique. *Eur Spine J* 2010; 19(6): 1010-1020.
5. Jiang S and Li W. Biomechanical study of proximal adjacent segment degeneration after posterior lumbar interbody fusion and fixation: a finite element analysis. *J Orthop Surg Res* 2019; 14(1): 135.
6. Van Rijsbergen M, Van Rietbergen B, Barthelemy V, et al. Comparison of patient-specific computational models vs. clinical follow-up, for adjacent segment disc degeneration and bone remodelling after spinal fusion. *PLoS ONE* 2018; 13(8): 1–24.
7. Castellvi AE and Andrew SA. Scient'x IsoBar TTL dynamic rod stabilization. *Motion Preservation Surgery of the Spine*. 3rd ed. Philadelphia: Saunders Elsevier, 2008, pp. 483-9.
8. Park P, Garton HJ, Gala VC, et al. Adjacent segment disease after lumbar or lumbosacral fusion: review of the literature. *Spine* 2004; 29:1938–1944.
9. Rahm MD and Hall BB. Adjacent segment degeneration after lumbar fusion with instrumentation: a retrospective study. *J Spinal Disord* 1996; 9: 392–400.
10. Más Y, Gracia L, Ibarz E, at al. Finite element simulation and clinical followup of lumbar spine biomechanics with dynamic fixations. *PLoS ONE* 2017; 12(11).
11. Mageswaran P, Techy F, Colbrunn RW, et al. Hybrid dynamic stabilization: a biomechanical assessment of adjacent and supraadjacent levels of the lumbar spine. *J Neurosurg Spine* 2012; 17(3): 232-242.
12. Maserati MB, Tormenti MJ, Panczykowski DM, et al. The use of a hybrid dynamic stabilization and fusion system in the lumbar spine: preliminary experience. *Neurosurg Focus* 2010; 28(6): E2.
13. Breau C, Shirazi-Adl A and De Guise J. Reconstruction of a human ligamentous lumbar spine using CT images-a three-dimensional finite element mesh generation. Annals of Biomedical Engineering 1991; 19(3): 291-302.
14. Liebschner MA, Kopperdahl DL, Rosenberg WS, et al. Finite element modeling of the human thoracolumbar spine. *Spine* 2003; 28(6): 559-565.
15. Castro APG, Paul CPL, Detiger SEL, et al. Long-Term Creep Behavior of the Intervertebral Disk: Comparison between Bioreactor Data and Numerical Results. *Front Bioeng Biotechnol* 2014; 2(November): 56.
16. Costa MC, Tozzi G, Cristofolini L, et al. Micro Finite Element models of the vertebral body: Validation of local displacement predictions. *PloS one* 2017; 12(7): e0180151.
17. Goel VK, Mehta A, Jangra J, et al. Anatomic facet replacement system (AFRS) restoration of lumbar segment mechanics to intact: a finite element study and in vitro cadaver investigation. *Int J Spine Surg* 2007; 1(1): 46-54.
18. Ayturk UM and Puttlitz CM. Parametric convergence sensitivity and validation of a finite element model of the human lumbar spine. *Comput Methods Biomech Biomed Engin* 2011; 14(8): 695-705.
19. Kiapour A, Ambati D, Hoy RW, et al. Effect of graded facetectomy on biomechanics of Dynesys dynamic stabilization system. *Spine* 2012; 37(10): 581-589.
20. Dreischarf M, Zander T, Shirazi-Adl A, et al. Comparison of eight published static finite element models of the intact lumbar spine: predictive power of models improves when combined together. *J Biomech* 2014; 47(8): 1757-1766.
21. Lee CH, Hsu CC and Chaing L. An Optimization Study for the Bone-Implant Interface Performance of Lumbar Vertebral Body Cages Using a Neurogenetic Algorithm and Verification Experiment. *J Med Biol Eng* 2018; 38(1): 22–32.
22. Malandrino A, Noailly J and Lacroix D. Numerical exploration of the combined effect of nutrient supply, tissue condition and deformation in the intervertebral disc. *J Biomech* 2014; 47(6): 1520-1525.
23. Putzer M, Ehrlich I, Rasmussen J, et al. Sensitivity of lumbar spine loading to anatomical parameters. *Journal of Biomechanics* 2016; 49(6): 953-958.

24. Busscher I, Ploegmakers JJ, Verkerke GJ, et al. Comparative anatomical dimensions of the complete human and porcine spine. *Eur Spine J* 2010; 19(7): 1104-1114.
25. Dao TT, Pouletaut P, Lazáry Á, et al. Multimodal Medical Imaging Fusion for Patient Specific Musculoskeletal Modeling of the Lumbar Spine System in Functional Posture. *J Med Biol Eng* 2017; 37(5): 739–749.
26. Dall'Ara E, Schmidt R, Pahr D, et al. A nonlinear finite element model validation study based on a novel experimental technique for inducing anterior wedge-shape fractures in human vertebral bodies in vitro. *J Biomech* 2010; 43(12): 2374–2380.
27. Chen CS, Cheng CK, Liu CL, et al. Stress analysis of the disc adjacent to interbody fusion in lumbar spine. *Med Eng Phys* 2001; 23(7): 485-493.
28. Erbulut DU, Zafarparandeh I, Hassan CR, et al. Determination of the biomechanical effect of an interspinous process device on implanted and adjacent lumbar spinal segments using a hybrid testing protocol: a finite-element study. *Journal of Neurosurgery: Spine* 2015; 23(2); 200-208.
29. Liu CL, Zhong ZC, Shih SL, et al. Influence of Dynesys system screw profile on adjacent segment and screw. *Clin Spine Surg* 2010; 23(6): 410-417.
30. Liu CL, Zhong ZC, Hsu HW, et al. Effect of the cord pretension of the Dynesys dynamic stabilisation system on the biomechanics of the lumbar spine: a finite element analysis. *Eur Spine J* 2011; 20(11): 1850-1858.
31. Chen CS, Huang CH and Shih SL. Biomechanical evaluation of a new pedicle screw-based posterior dynamic stabilization device (Awesome Rod System)-a finite element analysis. BMC *Musculoskelet Disord* 2015; 16(1): 81.
32. Lin HM, Pan YN, Liu CL, et al. Biomechanical comparison of the K-ROD and Dynesys dynamic spinal fixator systems–a finite element analysis. *Bio-Med Mater Eng* 2013; 23(6): 495-505.
33. Kim HJ, Chun HJ, Kang KT, et al. The biomechanical effect of pedicle screws' insertion angle and position on the superior adjacent segment in 1 segment lumbar fusion. *Spine* 2012; 37(19): 1637-1644.
34. Dreischarf M, Schmidt H, Putzier M, et al. Biomechanics of the L5–S1 motion segment after total disc replacement–Influence of iatrogenic distraction, implant positioning and preoperative disc height on the range of motion and loading of facet joints. *J Biomech* 2015; 48(12): 3283-3291.
35. Ruberté LM, Natarajan RN, and Andersson GB. Influence of single-level lumbar degenerative disc disease on the behavior of the adjacent segments—a finite element model study. *J Biomech 2009*; 42(3): 341-348.
36. Strube P, Tohtz S, Hoff E, et al. Dynamic stabilization adjacent to single-level fusion: part I. Biomechanical effects on lumbar spinal motion. *Eur Spine J* 2010; 19(12): 2171-2180.
37. Shin DS, Lee K and Kim D. Biomechanical study of lumbar spine with dynamic stabilization device using finite element method. *Comput Aided Des* 2007; 39(7): 559-567.
38. Rohlmann A, Zander T, Rao M, et al. Realistic loading conditions for upper body bending. *J Biomech* 2009; 42: 884–890.
39. Noailly J, Lacroix D and Planell JA. Finite element study of a novel intervertebral disc substitute. *Spine* 2005; 30(20): 2257-2264.
40. Zhong ZC, Wei SH, Wang JP, et al. Finite element analysis of the lumbar spine with a new cage using a topology optimization method. *Med Eng Phys* 2006; 28(1): 90-98.
41. AZO Materials. https://www.azom.com/properties.aspx?ArticleID=920 (accessed 19 November 2019).
42. Biswas JK, Rana M, Majumder S, et al. Effect of two-level pedicle-screw fixation with different rod materials on lumbar spine: A finite element study. *J Orthop Sci* 2018; 23(2): 258-265.
43. Yamamoto ISAO, Panjabi MM, Crisco TREY, et al. Three-dimensional movements of the whole lumbar spine and lumbosacral joint. *Spine* 1989; 14(11): 1256-1260.
44. Schmoelz W, Huber JF, Nydegger T, et al. Dynamic stabilization of the lumbar spine and its effects on adjacent segments: an in vitro experiment. *Spine* 2003; 28: 418-423.
45. Niosi CA, Zhu QA, Wilson DC, et al. Biomechanical characterization of the three-dimensional kinematic behaviour of the Dynesys dynamic stabilization system: an in vitro study. *Eur Spine J* 2006; 15(6): 913-922.
46. Cheng BC, Gordon J, Cheng J, et al. Immediate biomechanical effects of lumbar posterior dynamic stabilization above a circumferential fusion. *Spine* 2007; 32(23): 2551-2557.
47. Herren C, Beckmann A, Meyer S, et al. Biomechanical testing of a PEEK-based dynamic instrumentation device in a lumbar spine model. *Clin Biomech* 2017; 44: 67-74.
48. Rohlmann A, Neller S, Bergmann G, et al. Effect of an internal fixator and a bone graft on intersegmental spinal motion and intradiscal pressure in the adjacent regions. *Eur Spine J* 2001; 10(4): 301-308.
49. Wilke HJ, Drumm J, Häussler K, et al. Biomechanical effect of different lumbar interspinous implants on flexibility and intradiscal pressure. *European Spine Journal* 2008; 17(8): 1049-1056.
50. Heuer F, Schmidt H, Claes L, et al. Stepwise reduction of functional spinal structures increase vertebral translation and intradiscal pressure. *J Biomech* 2007; 40(4): 795-803.
51. Niinomi M. Mechanical properties of biomedical titanium alloys. *Mater. Sci. Eng. A* 1998; 243(1-2): 231-236.

52. Geringer J, Tatkiewicz W and Rouchouse G. Wear behavior of PAEK, poly (aryl-ether-ketone), under physiological conditions, outlooks for performing these materials in the field of hip prosthesis. *Wear* 2011; 271(11-12): 2793-2803.
53. Eberlein R, Holzapfel GA and Fröhlich M. Multi-segment FEA of the human lumbar spine including the heterogeneity of the annulus fibrosus. *Comput Mech* 2004; 34(2): 147-163.
54. Frzell P, Hägg O, Wessberg P, et al. 2001 Volvo Award Winner in Clinical Studies: Lumbar fusion versus nonsurgical treatment for chronic low back pain: a multicenter randomized controlled trial from the Swedish Lumbar Spine Study Group. *Spine* 2001; 26(23): 2521-2532.
55. Miyakoshi N, Abe E, Shimada Y, et al. Outcome of one-level posterior lumbar interbody fusion for spondylolisthesis and postoperative intervertebral disc degeneration adjacent to the fusion. *Spine* 2000; 25(14): 1837-1842.
56. Ishihara H, Osada R, Kanamori M, et al. Minimum 10-year follow-up study of anterior lumbar interbody fusion for isthmic spondylolisthesis. *Clin Spine Surg* 2001; 14(2): 91-99.
57. Glaser J, Stanley M, Sayre H, et al. A 10-year follow-up evaluation of lumbar spine fusion with pedicle screw fixation. *Spine* 2003; 28(13): 1390-1395.
58. Castelli R and Steverlynck A. Hybrid constructions of the lumbosacral spine: preliminary work-20 cases. *Coluna/Columna* 2013; 12(4): 300-303.
59. Kashkoush A, Agarwal N, Paschel E, et al. Evaluation of a hybrid dynamic stabilization and fusion system in the lumbar spine: a 10 year experience. *Cureus* 2016; 8(6).
60. Lee SE, Jahng TA and Kim HJ. Hybrid surgery combined with dynamic stabilization system and fusion for the multilevel degenerative disease of the lumbosacral spine. *Int J Spine Surg* 2015; 9: 45.
61. Baioni A, Di Silvestre M, Greggi T, et al. Does hybrid fixation prevent junctional disease after posterior fusion for degenerative lumbar disorders? A minimum 5-year follow-up study. *Eur Spine J* 2015; 24(7): 855-864.
62. Formica M, Cavagnaro L, Basso M, et al. Is it possible to preserve lumbar lordosis after hybrid stabilization? Preliminary results of a novel rigid–dynamic stabilization system in degenerative lumbar pathologies. *Eur Spine J* 2015; 24(7): 849-854.
63. Schmoelz W, Huber JF, Nydegger T, et al. Influence of a dynamic stabilisation system on load bearing of a bridged disc: an in vitro study of intradiscal pressure. *Eur Spine J* 2006; 15(8): 1276-1285.
64. Oikonomidis S, Ashqar G, Kaulhausen T, et al. Clinical experiences with a PEEK-based dynamic instrumentation device in lumbar spinal surgery: 2 years and no more. *J Orthop Surg Res* 2018; 13(1): 196.